Published in final edited form as:
Bone. 2007 September ; 41(3): 331–339. doi:10.1016/j.bone.2007.05.009.

For submission to BONE: Bone mass is inversely proportional to *Dkk1* levels in mice

Bryan T MacDonald[1], **Danese M Joiner**[2], **Sivan M Oyserman**[2], **Parul Sharma**[3], **Steven A Goldstein**[2], **Xi He**[1], and **Peter V Hauschka**[3]

Bryan T MacDonald: bryan.macdonald@childrens.harvard.edu; Danese M Joiner: speededj@umich.edu; Sivan M Oyserman: oyserman@umich.edu; Parul Sharma: parul.sharma@childrens.harvard.edu; Steven A Goldstein: stevegld@umich.edu; Xi He: xi.he@childrens.harvard.edu; Peter V Hauschka: peter.hauschka@childrens.harvard.edu

[1] Division of Neuroscience, Children's Hospital, Harvard Medical School, Boston, MA 02115

[2] Orthopaedic Research Laboratories, Department of Orthopaedic Surgery, University of Michigan, Ann Arbor, MI 48109

[3] Department of Orthopedic Surgery, Children's Hospital, Harvard Medical School, Boston, MA 02115

Abstract

The Wnt/β-catenin signaling pathway has emerged as a key regulator in bone development and bone homeostasis. Loss-of-function mutations in the Wnt co-receptor *LRP5* result in osteoporosis and "activating" mutations in *LRP5* result in high bone mass. Dickkopf-1 (DKK1) is a secreted Wnt inhibitor that binds LRP5 and LRP6 during embryonic development, therefore it is expected that a decrease in DKK1 will result in an increase in Wnt activity and a high bone mass phenotype. $Dkk1^{-/-}$ knockout mice are embryonic lethal, but mice with hypomorphic $Dkk1^{d}$ (*doubleridge*) alleles that express low amounts of *Dkk1* are viable. In this study we generated an allelic series by crossing $Dkk1^{+/-}$ and $Dkk1^{+/d}$ mice resulting in the following genotypes with decreasing *Dkk1* expression levels: +/+, +/*d*, +/− and *d*/−. Using μCT imaging we scanned dissected left femora and calvariae from eight week old mice (n=60). We analyzed the distal femur to represent trabecular bone and the femur diaphysis for cortical endochondral bone. A region of the parietal bones was used to analyze intramembranous bone of the calvaria. We found that trabecular bone volume is increased in *Dkk1* mutant mice in a manner that is inversely proportional to the level of *Dkk1* expression. Trabeculae number and thickness were significantly higher in the low *Dkk1* expressing genotypes from both female and male mice. Similar results were found in cortical bone with an increase in cortical thickness and cross sectional area of the femur diaphysis that correlated with lower *Dkk1* expression. No consistent differences were found in the calvaria measurements. Our results indicate that the progressive *Dkk1* reduction increases trabecular and cortical bone mass and that even a 25% reduction in *Dkk1* expression could produce significant increases in trabecular bone volume fraction. Thus DKK1 is a negative regulator of normal bone homeostasis *in vivo*. Our study suggests that manipulation of DKK1 function or expression may have therapeutic significance for the treatment of low bone mass disorders.

Corresponding Author: Bryan MacDonald, Children's Hospital, Harvard Medical School, 320 Longwood Ave, Enders 470, Boston, MA 02115.

Keywords

Dickkopf1; Wnt/LRP5; bone; microcomputed tomography; mice

Introduction

During embryonic development and throughout adult life, Wnt signaling plays many roles to guide cell identity, polarity and proliferation [1]. Wnts are an important regulator of stem cells, and disruption of the Wnt pathway can result in cancer [2]. Wnt/β-catenin signaling is initiated when a Wnt ligand binds to Frizzled and LDL receptor-related protein 5 or 6 (LRP5/6) to form a ternary complex, resulting in the stabilization of β-catenin, which accumulates in the cell and travels into the nucleus to activate the expression of Wnt target genes [3,4].

The identification of *LRP5* mutations in bone disorders linked the Wnt/β-catenin pathway to the field of bone biology. Loss-of-function mutations in *LRP5* were found in patients with osteoporosis-pseudoglioma (OPPG), a recessive disorder characterized by low bone density and persistent eye/vitreal vasculature [5]. Obligate carriers for the OPPG mutations are also more at risk for developing osteoporosis. The phenotype of *Lrp5*$^{-/-}$ knock-out mice was identical to the human OPPG disease and revealed an impairment in osteoblast proliferation [6]. The converse is found in patients with dominant "gain-of-function" mutations in *LRP5* which exhibit abnormally high bone density [7,8]. A transgenic mouse model carrying a human *LRP5* high bone mass mutation exhibited significant increases in bone density and mechanical properties [9,10]. Studies have shown that removing one *Lrp6* copy from *Lrp5*$^{-/-}$ mice increases the osteoporosis severity, suggesting that both *LRP5* and *LRP6* are critical determinants of bone mass [11].

Further studies using conditional removal or activation of β-catenin at different times during development have revealed multiple roles that the Wnt pathway plays in osteoblast proliferation and maturation [12]. The absence of β-catenin in early skeletal progenitor cells causes osteoblast precursors to become chondrocytes [13–15]. Inactivation of β-catenin in committed osteoblast progenitors prevented the expression of osteoblast-specific genes, indicating that β-catenin is also essential for osteoblast differentiation [15,16]. Mice with β-catenin removal in mature osteoblasts displayed severe osteopenia, which surprisingly was due to an increase in osteoclasts [17,18]. Normally, mature osteoblasts will secrete a RANKL decoy receptor, osteoprotegrin (OPG), to inhibit excess osteoclastogenesis [19]. OPG is a Wnt responsive target gene and was found to be reduced in β-catenin$^{-/-}$ osteoblasts and upregulated in cells with hyperactive Wnt signaling [17,18,20]. Therefore the Wnt/β-catenin pathway directly controls multiple steps of osteoblast development, and indirectly controls osteoclast differentiation through OPG secreted from osteoblasts.

Wnt signaling is modulated by several families of secreted inhibitors, which bind either competitively to the Wnt ligand, such as sFRP, or directly to the LRP5/6 receptor (SOST and Dkks) [21]. Consistent with the removal of a Wnt inhibitor, the mouse knockout for *Sfrp1*$^{-/-}$ displays an increase in trabecular bone mass in adult animals [22]. Previously identified as a BMP antagonist, SOST also binds to LRP5 and LRP6 in the extracellular region and antagonizes Wnt signaling [23,24]. *SOST* loss-of-function mutations are responsible for Sclerosteosis, a human disorder characterized by increased bone density and excessive bone overgrowth [25,26]. A subset of SOST mutations are caused by a deletion of a 52-kb downstream regulatory region in patients with Van Buchem disease [27,28]. Sclerosteosis and Van Buchem disease are highly similar to LRP5 high bone mass disorders suggesting a possible molecular link [4]. Indeed our recent study suggests that SOST binding is diminished in LRP5 high bone mass mutations, resulting in SOST-resistant LRP5 receptors [29].

Dickkopf-1 (DKK1) was identified as an inhibitor of the canonical Wnt pathway in early vertebrate embryonic patterning [30]. DKK1 binds to LRP5 and LRP6, reducing their availability to form a complex with Wnt and Frizzled [31–34]. *Dkk1*$^{-/-}$ knockout mice display severe head formation defects, polydactyly, vertebral fusions and die shortly after birth [35]. Another *Dkk1* mutant caused by a distant transgenic insertion results in reduced *Dkk1* expression in the *doubleridge* mouse (referred to as *Dkk1*^{d}) [36,37]. The residual *Dkk1* expression in *Dkk1*$^{d/d}$ or *Dkk1*$^{d/-}$ mice is sufficient for head development and survival to adulthood. In addition to being widely and dynamically expressed during embryonic development, *Dkk1* is also predominantly expressed in adult bone tissues [38,39]. Similar to the expression of *SOST*, *Dkk1* is present in the mature osteoblast/osteocyte, suggesting that DKK1 may regulate bone homeostasis [40]. In contrast to *SOST* and *Dkk1*, *Dkk2* is expressed in the early osteoblast and is down-regulated as the osteoblast matures. Mice deficient for *Dkk2* are osteopenic due to a failure in osteoblast maturation [41]. While this manuscript was in preparation, a study of *Dkk1*$^{+/-}$ mutant mice demonstrated that the removal of one *Dkk1* allele results in an increase in bone mass [42]. In our study we utilized mice with hypomorphic and null *Dkk1* mutant alleles to genetically titrate *Dkk1* expression levels over a broad range. Here we show that peak bone mass in mice is inversely proportional to the level of *Dkk1* expression *in vivo*.

Materials and Methods

Dkk1 mutant mice

Hypomorphic *Dkk1*^{d} mice and knock-out *Dkk1*$^{-}$ mice were maintained on the C3HeB/FeJ strain background. For the microCT study, femora and calvariae were collected from eight week old animals from 15 litters of *Dkk1*$^{+/-}$ and *Dkk1*$^{+/d}$ breeding. Eight animals were used for each sex/genotype group, with the exception of the female *Dkk1*$^{d/-}$ group. Malocclusion was more common in females than in males, resulting in the survival of fewer female *Dkk1*$^{d/-}$ animals (n=4). Animals were genotyped at the *Dkk1*^{d} and *Dkk1*$^{-}$ loci as previously described [37].

RT-PCR

For this experiment a total of 30 newborn pups (postnatal day 3) were obtained from 4 litters. Neonatal calvariae were dissected and stripped of loosely bound underlying tissue. RNA was extracted using the RNeasy Mini Isolation kit with the QIAshredder columns (Qiagen), and equal amounts of total RNA were used to prepare oligo dT primed cDNA using the “Ready-To-Go You-Prime First-Strand Beads (Amersham Biosciences). The following RT-PCR primers were used: mDKK1-3exF (GAATATGCATGCCCTCTGAC), mDKK1-4exR (TCAGTGTGGTTCTTCTGGGA), mDKK1-2exF (ATGAGGCACGCTATGTGCT), mDKK1-3exR (CGTTGTGGTCATTACCAAGG), mDKK2 F (CAGTCACTGAGAGCATCCTCA), mDKK2 R (CCTGATGGAGCACTGGTTTGC), mHPRT-F1 (TCAAGGGCATATCCAACAACAAAC), mHPRT-R1 (AGCAGTACAGCCCCAAAATGGTTA). Quantitative RT-PCR was performed using the SYBR Green PCR Master Mix kit (Applied Biosystems) and run on an ABI7700 machine. One outlier +/+ sample was eliminated from the analysis, leaving the following samples sizes: +/+ n=7, +/*d* n=12, +/− n=4, *d*/− n=6. Relative gene expression levels were calculated as described [43].

MicroCT

Femora from 8 week old mice were dissected, cleaned of soft tissue and fixed overnight in 10% neutral buffered formalin and stored in 70% ethanol. Left femora were scanned by a cone beam μCT system (GE Healthcare BioSciences), and reconstructed at a voxel size of 18 microns. Cortical geometric analyses for cortical thickness, cross sectional area (CSA),

bending moment of inertia for the medial-lateral axis (Iyy) and tissue mineral density (TMD) were performed on a 3 mm mid-diaphyseal femoral segment as previously described [44]. A standardized volume of trabecular bone was segmented using a spline algorithm starting at the distal growth plate and moving proximal for a total of 20% of the total femur length. The elements of the spline were interpolated to generate a 3D region of interest (ROI) which was used for trabecular analyses to measure bone volume fraction (BVF), trabecular thickness, trabecular number, trabecular spacing and TMD. The ROI for the calvaria was a 3mm segment to the right of the sagittal and between the coronal and lambdoid sutures created with the standard ROI tool and used to measure cortical thickness, CSA, bone mineral density (BMD) and TMD. Note: one male +/+ (n= 7) and one male +/*d* (n=7) were unavailable for calvaria scanning.

Stastical Analysis

All results are expressed as the mean±SD. Post Hoc multiple comparison tests were conducted with SPSS software on analyzed parameters and p values less than 0.05 were considered significant. For all data, * indicates $p<0.05$ (95% confidence interval) and ** indicates $p<0.01$ (99% confidence interval) compared to +/+ sex matched controls.

Results

To study the effects of reduced *Dkk1* levels in bone, we utilized the *Dkk1* knock-out (*Dkk1*$^{-}$) and transgene insertional hypomorph (*Dkk1*^{d}) mutant alleles to genetically titrate the *Dkk1* expression levels. Heterozygous *Dkk1*$^{+/-}$ and *Dkk1*$^{+/d}$ were mated to produce offspring of the following genotypes with decreasing *Dkk1* expression levels: +/+, +/*d*, +/− and *d*/−. Previously, the *Dkk1* expression from *Dkk1*$^{+/-}$ calvaria cells was reported to be approximately 50% of wild-type levels, suggesting the remaining wild-type *Dkk1* allele is independently regulated and unable to compensate for the deleted allele [42]. During embryonic development, *Dkk1* expression from the *Dkk1*^{d} allele varied from 1–34% of the normal transcriptional level depending on the embryo age and tissue examined [37]. To evaluate the reduced *Dkk1* expression in postnatal bone from our *Dkk1* mutant mice, we performed quantitative RT-PCR from postnatal day 3 (P3) calvaria RNA. The results indicate that *Dkk1* is expressed at 25% of wild-type levels in the *Dkk1*$^{d/-}$ compound heterozygote bone. (Fig. 1) Additionally *Dkk1* expression in the heterozygous *Dkk1*$^{+/d}$ calvaria was approximately 75%, consistent with the hypomorphic allele contributing only 25% of wild-type levels. The relative expression level of the *Dkk1*$^{+/-}$ was higher than expected at 59%, possibly due to the small sample size of this group (n=4). *Dkk1* expression results were confirmed using a second *Dkk1* primer set, and the expression level of another related family member, *Dkk2*, was not altered in any of the *Dkk1* mutants examined consistent with previous reports (data not shown) [42].

Dkk1$^{+/-}$ and *Dkk1*$^{+/d}$ animals appear normal and do not display any visible phenotype. Although *Dkk1*$^{d/-}$ animals are viable, they consistently display microphthalmia, forelimb polydactyly and vertebral fusions in the caudal vertebrae. Some of the *Dkk1*$^{d/-}$ mice have mandibular defects that result in misalignment of the front incisors, however the animals with severe malocclusions were not used in this study. Femora and calvariae were dissected from 8-week old mice and the left femora and parietal bone regions were used for microCT scans. Animal weights were not significantly different between females; however the male *Dkk1*$^{d/-}$ mice weighed significantly less than the wild-type males. (Table 1)

Grossly the femora from *Dkk1*$^{d/-}$ mice appeared morphologically different. The third trochanter, normally associated as the insertion site for the gluteus maximus, was shifted distally and extended along the lateral edge into the diaphysis. (Fig 2A-D) Additionally all *Dkk1*$^{d/-}$ femora exhibited a 0.3–0.5 mm wide fibrous ligament-like structure that ran from the distal, posterior edge of the third trochanter to the lateral sesamoid bone and attached to the

lateral condyle of the femur. This accessory ligament was thinner in the *Dkk1*$^{d/-}$ females and also in the smaller *Dkk1*$^{d/-}$ males by weight. Examination of *Dkk1*$^{+/-}$ and *Dkk1*$^{+/d}$ femora revealed a thin <0.1 mm fibrous element in a similar location, however this structure was loosely attached and could easily be pulled away from the bone. The femora from *Dkk1*$^{+/+}$ mice did not have this fibrous element. The distally shifted third trochanter and accessory ligament in the *Dkk1*$^{d/-}$ femur is similar to the *Hoxa10*$^{-/-}$ limb phenotype [45]. However, unlike the severely affected *Hoxa10*$^{-/-}$ mutants, the knee joint and surrounding sesamoid bones were not affected in the *Dkk1*$^{d/-}$ mice.

To quantify the geometric differences in the *Dkk1* mutants, femur length and third trochanter position were measured from the microCT scans. (Table 1) The average femur length was significantly lower in the *Dkk1*$^{d/-}$ males, consistent with the decreased weight in this group. To determine the third trochanter position relative to the total femur length, the ratio of femur length to the vertical distance of the third trochanter was calculated. This revealed significant differences between the wild type and *Dkk1* mutant femora, particularly in the male mice.

To examine the properties of the cortical bone, a 3 mm region of the femur mid-diaphysis was analyzed using a previously described method [44]. Compared to the wild-type controls, cortical thickness and cross sectional area were significantly increased in the *Dkk1*$^{+/-}$ and even more so in the *Dkk1*$^{d/-}$ samples. (Table 2) The calculated moment of inertia for the medial-lateral axis (Iyy) was used as an estimate of the mechanical properties of the femur and significant increases were found in the female *Dkk1*$^{d/-}$ and the male *Dkk1*$^{+/-}$ and *Dkk1*$^{d/-}$ samples. No changes were detected in tissue mineral density, suggesting that the degree of mineralization of cortical bone within the area analyzed was equivalent between the sex matched groups. Cross section alpha blends of the mid-diaphysis illustrate the increase in voxel density in the *Dkk1*$^{+/-}$ and *Dkk1*$^{d/-}$ mice. (Fig. 2E–J) Trabeculation within the marrow space was commonly observed in the *Dkk1*$^{d/-}$ male femora.

To evaluate the alterations in trabecular bone from the *Dkk1* mutant mice, a region of the distal femur was used for the trabecular analysis. (Fig. 3A-H) Measurements of bone volume fraction show significant increases in all *Dkk1* mutant mice compared to wild-type controls. (Table 3) Furthermore the incremental increases in bone volume fraction within the geneotypes (+/+ < +/*d* < +/− < *d*/−) indicate an inversely proportional relationship to *Dkk1* expression levels. Significant increases in trabecular thickness were found in the *Dkk1*$^{+/-}$ and even more so in *Dkk1*$^{d/-}$ mice, compared to sex matched wild-type controls. Trabecular number was also increased and trabecular spacing decreased, further supporting the measured overall increase in trabecular mass with progressively lower levels of *Dkk1* expression. Tissue mineral density was unchanged between most of the groups, with the exception of the *Dkk1*$^{+/-}$ males which displayed a decrease in mineralization. Taken together with the increase in trabecular bone mass for the *Dkk1*$^{+/-}$ males, it is likely that a higher proportion of more recently formed trabecular bone is present within this group. Measurements from the trabecular analysis plotted using the *Dkk1* expression levels of *d*/− = 25%, +/− = 50%, +/*d* = 75%, +/+ = 100% graphically demonstrate the correlation between *Dkk1* dosage and trabecular bone properties. (Fig. 3I–L)

To examine the properties of intramembranous bone, a coronal section of the parietal bones was used to measure cortical thickness and cross sectional area. A 3mm segment to the right of the sagittal and between the coronal and lambdoid sutures, encompassing most of the right parietal bone was used to measure BMD and TMD. No significant increases or decreases in calvaria bone properties were detected between *Dkk1* mutant mice and wild-type, sex-matched controls. (Table 4) However, significant increases ($p<0.05$) were present in cortical thickness and BMD between *Dkk1*$^{+/d}$ and *Dkk1*$^{+/-}$ males and in CSA between *Dkk1*$^{+/d}$ and *Dkk1*$^{d/-}$ females, although these significant differences may be explained by the lower variation from the *Dkk1*$^{+/d}$ samples compared to the relatively high variation found in the other genotype

groups. In summary, there are no observable trends that associate *Dkk1* dosage with alterations in the intramembranous bone of the calvaria.

Discussion

In this study we have examined the bone phenotype of adult mice with genetically reduced *Dkk1* levels. The data from the microCT analysis indicate that dose-dependent decreases in *Dkk1* expression cause 1) alterations in femur shape, 2) increases in cortical thickness and cross sectional area, 3) increases in trabecular bone volume and trabecular number, and 4) no consistent changes in the intramembranous bone of the calvaria. This work supports the growing body of literature reporting the Wnt pathway as an important determinant of bone mass.

To date there have been no reported human mutations in *DKK1*, although null mutations would most likely be incompatible with life due to the early requirement of DKK1 during embryonic head induction. Nonetheless, our findings suggest that even a 25% reduction of *DKK1* expression will produce significant increases in trabecular bone mass. It is possible that reduced *DKK1* levels (or activity) will resemble Van Buchem disease, a high bone mass disorder caused by reduced *SOST* expression. Both DKK1 and SOST act through LRP5/6 to inhibit Wnt/β-catenin signaling and both are expressed in mature osteoblasts and osteocytes suggesting a similar biological role in bone homeostasis [24]. In addition, the hypomorphic $Dkk1^{d}$ allele bears a resemblance to the Van Buchem mutation that affects *SOST* expression. The $Dkk1^{d}$ mutation is a 60 kb deletion at the transgene insertion site which is located over 150 kb downstream from the *Dkk1* gene and the Van Buchem disease mutation results from a 52-kb deletion of a regulatory region that is 35 kb downstream from *SOST* [46]. It is unknown if the reduced expression from the $Dkk1^{d}$ allele is due to transgene induced silencing or the deletion of a regulatory element [37]. However, our study implies that a human high-bone mass disorder originating from hypomorphic mutations at the *DKK1* locus or within the surrounding genomic region is probable.

$Dkk1^{d/-}$ mice display forelimb and hindlimb polydactyly, but since no skeletal abnormalities were observed in the stylopod structures (humerus or femur) of newborn mice, we chose femora for the microCT study. However, we now report that the adult femora of $Dkk1^{d/-}$ mice exhibit a distal shift in the third trochanter and an accessory ligament that runs along the lateral edge connecting the third trochanter to the lateral condyle of the femur. These irregular structures were less pronounced in the smaller female and male $Dkk1^{d/-}$ mice suggesting that either size or weight influences this phenotype. Additionally, slight changes in third trochanter location in $Dkk1^{+/-}$ and $Dkk1^{+/d}$ mice, and a thin fibrous element along the lateral femur, indicate that phenotype severity is related to *Dkk1* dosage. Curiously, a distally shifted third trochanter and ectopic ligament is also found in $Hoxa10^{-/-}$ mice, and the $Dkk1^{d/-}$ femora are remarkably similar to the mildly affected $Hoxa10^{-/-}$ mice on an inbred 129/Sv background [45]. The paralogous *Hox10* genes are responsible for patterning the stylopod and stylopod/zeugopod junction (elbow and knee joints), particularly in the hindlimb [47]. *Favier et al* speculate that the ectopic ligament in $Hoxa10^{-/-}$ originates from a thickening of the septum intermuscularis femoris lateralis, and the abnormal thickening of this structure may be due to the antagonistic tensions between the gastocnemius and the gluteus superficialis muscles [45]. As a result, the third trochanter is subject to an alteration in forces generated by the gastrocnemius which could cause the remodeling and distal displacement of this tuberosity. In contrast to the *Dkk1* and *Hoxa10* mutants, mice deficient for myostatin ($Gdf8^{-/-}$), a negative regulator of muscle mass, display a *proximal* displacement and enlargement of the third trochanter due to the increased forces from an enlarged gluteus maximus [48]. This further suggests that the third trochanter is subject to remodeling in the adult mouse, and displacement of the third trochanter in the *Dkk1* mutant femora is a mechano-response to loads imparted from a distal muscle of the

hindlimb. However, we would like to note that in the *Dkk1*$^{d/-}$ mutants, the distal edge of the third trochanter extends into the mid-diaphyseal region used to analyze the cortical bone traits. This adds further complexity to the cortical bone geometry for these animals and may affect our conclusions regarding the *Dkk1*$^{d/-}$ cortical bone phenotype.

The *Dkk1* mutant mice used in the study were maintained on a C3H background. During the original characterization of the *doubleridge* mouse (*Dkk1*$^{d/d}$), we observed a higher incidence of anterior head malformations in mice from the C57BL/6 (B6) strain compared with C3H *Dkk1* mutants [37]. Furthermore, *Dkk1*$^{d/-}$ mice are not viable on the B6 background (BTM unpublished observation) which necessitated a different strain background in order to study the adult bone phenotype. Recently the high bone mass phenotype of the *Dkk1*$^{+/-}$ heterozygote was described using mice on the B6 background [42]. Bone density varies greatly among the mouse inbred strains, particularly between the C3H and B6 strains. Total density is approximately 50% higher in C3H femora compared to B6, and cortical bone properties are consistently higher in C3H mice [49,50]. Osteoblasts from C3H mice exhibit higher alkaline phosphatase activity and greater mineralization compared to cultured B6 osteoblasts, which contributes to the increased bone formation rate observed in the C3H inbred strain [51]. Nevertheless, our study concludes that even on a higher bone density mouse strain like C3H, reduction of *Dkk1* is able to significantly increase bone mass. In addition, we also observed sex-specific differences in our 8-week old bone samples on the C3H background. Measurements of cortical bone were higher in males, whereas trabecular BVF and trabecular thickness were higher in females. Yet compared to sex-matched wild-type controls, the relative changes in bone properties were consistent between females and males in the *Dkk1* mutant mice (Fig. 2,3). *Morvan et al* examined the tibiae from 12 week old B6 mice and did not find any sex differences in their samples; and in their study male and female samples were analyzed together [42]. However the sex-specific differences may be smaller in the low bone density B6 background. Due to the differences in mouse strain background, it is difficult to directly compare the relative increases in bone properties from the heterozygous *Dkk1*$^{+/-}$ mice between our studies. However in our study we have uncovered the unique bone phenotype of the *Dkk1*$^{d/-}$ hypomorph/null and our examination of the *Dkk1*$^{+/d}$ mice expressing 75% of the normal *Dkk1* levels reveals the minimum *Dkk1* reduction needed to produce significant changes in trabecular bone mass.

Due to high variation in the calvaria measurements, we are unable to determine what effect *Dkk1* reduction has on intramembranous bone with our current sample sizes. In addition to the bone apposition differences between endochondral and intramembranous bone, the parietal bones are exposed to very different and less dynamic mechanical loading patterns than the femora [51]. A recent study has shown that osteoblasts from *Lrp5*$^{-/-}$ mice are defective for mechanotransduction and fail to synthesize bone matrix after mechanical loading [52]. Therefore, the reduction of a Wnt inhibitor such as DKK1 should result in an increased LRP5-mediated osteogenic response to mechanical stress. This may explain why dramatic changes in bone properties were only found in the limb bones that are subjected to large variations in repetitive mechanical loading. Presently, the lack of strong evidence of increased calvaria BMD suggests that *Dkk1* deficiency may not result in the severe craniosynsystosis present in the *SOST* loss of function diseases.

It is unknown if LRP6 is critical for mechanotransduction in the osteoblast. LRP6 plays an essential role during embryogenesis and the severe developmental defects in *Lrp6*$^{-/-}$ mice prevent the study of postnatal bone [53]. However, heterozygous *Lrp6*$^{+/-}$ and hypomorphic *ringelshwanz Lrp6* mutant mice exhibit delays in ossification and decreased bone mass in adults [11,54]. Recently a human *LRP6* mutation was reported in a family with coronary artery disease and osteoporosis, further suggesting that loss of function *LRP6* mutations result in low bone mass [55]. In contrast, the hypermorphic *Crooked tail Lrp6* mouse mutant is caused by a

missense mutation that prevents DKK1 mediated Wnt inhibition, though the adult bone phenotype was not examined in the *Lrp6*$^{Cd/+}$ mice [56]. Further studies are required to determine if LRP6 performs the same role as LRP5 in adult bone and if DKK1 inhibits these receptors differentially during osteogenesis. In summary, our study using the genetic reduction of *Dkk1* in mice illustrates the importance of regulating the Wnt pathway in bone homeostasis and highlights the therapeutic potential of targeting DKK1 in low bone mass disorders.

Acknowledgments

Hypomorphic *Dkk1*^{d} and *Dkk1* null mice were generously provided by M Meisler and H Westphal, respectively. This work was supported by NIH GM073357 (BTM), NSF Graduate Student Research Fellowship (DMJ), NIH AR046024 (SAG), NIH GM057603 (XH) and the St. Giles Foundation (PVH).

Funding sources supporting the study: NIH GM073357 (BTM), NSF Graduate Student Research Fellowship (DMJ), NIH AR046024 (SAG), NIH GM057603 (XH) and St. Giles Foundation (PVH)

References

1. Nusse R. Wnt signaling in disease and in development. Cell Res 2005;15:28–32. [PubMed: 15686623]
2. Reya T, Clevers H. Wnt signalling in stem cells and cancer. Nature 2005;434:843–50. [PubMed: 15829953]
3. Tamai K, Semenov M, Kato Y, Spokony R, Liu C, Katsuyama Y, Hess F, Saint-Jeannet JP, He X. LDL-receptor-related proteins in Wnt signal transduction. Nature 2000;407:530–5. [PubMed: 11029007]
4. He X, Semenov M, Tamai K, Zeng X. LDL receptor-related proteins 5 and 6 in Wnt/beta-catenin signaling: arrows point the way. Development 2004;131:1663–77. [PubMed: 15084453]
5. Gong Y, Slee RB, Fukai N, Rawadi G, Roman-Roman S, Reginato AM, Wang H, Cundy T, Glorieux FH, Lev D, Zacharin M, Oexle K, Marcelino J, Suwairi W, Heeger S, Sabatakos G, Apte S, Adkins WN, Allgrove J, Arslan-Kirchner M, Batch JA, Beighton P, Black GC, Boles RG, Boon LM, Borrone C, Brunner HG, Carle GF, Dallapiccola B, De Paepe A, Floege B, Halfhide ML, Hall B, Hennekam RC, Hirose T, Jans A, Juppner H, Kim CA, Keppler-Noreuil K, Kohlschuetter A, LaCombe D, Lambert M, Lemyre E, Letteboer T, Peltonen L, Ramesar RS, Romanengo M, Somer H, Steichen-Gersdorf E, Steinmann B, Sullivan B, Superti-Furga A, Swoboda W, van den Boogaard MJ, Van Hul W, Vikkula M, Votruba M, Zabel B, Garcia T, Baron R, Olsen BR, Warman ML. LDL receptor-related protein 5 (LRP5) affects bone accrual and eye development. Cell 2001;107:513–23. [PubMed: 11719191]
6. Kato M, Patel MS, Levasseur R, Lobov I, Chang BH, Glass DA 2nd, Hartmann C, Li L, Hwang TH, Brayton CF, Lang RA, Karsenty G, Chan L. Cbfa1-independent decrease in osteoblast proliferation, osteopenia, and persistent embryonic eye vascularization in mice deficient in Lrp5, a Wnt coreceptor. J Cell Biol 2002;157:303–14. [PubMed: 11956231]
7. Little RD, Carulli JP, Del Mastro RG, Dupuis J, Osborne M, Folz C, Manning SP, Swain PM, Zhao SC, Eustace B, Lappe MM, Spitzer L, Zweier S, Braunschweiger K, Benchekroun Y, Hu X, Adair R, Chee L, FitzGerald MG, Tulig C, Caruso A, Tzellas N, Bawa A, Franklin B, McGuire S, Nogues X, Gong G, Allen KM, Anisowicz A, Morales AJ, Lomedico PT, Recker SM, Van Eerdewegh P, Recker RR, Johnson ML. A mutation in the LDL receptor-related protein 5 gene results in the autosomal dominant high-bone-mass trait. Am J Hum Genet 2002;70:11–9. [PubMed: 11741193]
8. Boyden LM, Mao J, Belsky J, Mitzner L, Farhi A, Mitnick MA, Wu D, Insogna K, Lifton RP. High bone density due to a mutation in LDL-receptor-related protein 5. N Engl J Med 2002;346:1513–21. [PubMed: 12015390]
9. Babij P, Zhao W, Small C, Kharode Y, Yaworsky PJ, Bouxsein ML, Reddy PS, Bodine PV, Robinson JA, Bhat B, Marzolf J, Moran RA, Bex F. High bone mass in mice expressing a mutant LRP5 gene. J Bone Miner Res 2003;18:960–74. [PubMed: 12817748]
10. Akhter MP, Wells DJ, Short SJ, Cullen DM, Johnson ML, Haynatzki GR, Babij P, Allen KM, Yaworsky PJ, Bex F, Recker RR. Bone biomechanical properties in LRP5 mutant mice. Bone 2004;35:162–9. [PubMed: 15207752]

11. Holmen SL, Giambernardi TA, Zylstra CR, Buckner-Berghuis BD, Resau JH, Hess JF, Glatt V, Bouxsein ML, Ai M, Warman ML, Williams BO. Decreased BMD and limb deformities in mice carrying mutations in both Lrp5 and Lrp6. J Bone Miner Res 2004;19:2033–40. [PubMed: 15537447]
12. Hartmann C. A Wnt canon orchestrating osteoblastogenesis. Trends Cell Biol 2006;16:151–8. [PubMed: 16466918]
13. Hu H, Hilton MJ, Tu X, Yu K, Ornitz DM, Long F. Sequential roles of Hedgehog and Wnt signaling in osteoblast development. Development 2005;132:49–60. [PubMed: 15576404]
14. Hill TP, Spater D, Taketo MM, Birchmeier W, Hartmann C. Canonical Wnt/beta-catenin signaling prevents osteoblasts from differentiating into chondrocytes. Dev Cell 2005;8:727–38. [PubMed: 15866163]
15. Day TF, Guo X, Garrett-Beal L, Yang Y. Wnt/beta-catenin signaling in mesenchymal progenitors controls osteoblast and chondrocyte differentiation during vertebrate skeletogenesis. Dev Cell 2005;8:739–50. [PubMed: 15866164]
16. Rodda SJ, McMahon AP. Distinct roles for Hedgehog and canonical Wnt signaling in specification, differentiation and maintenance of osteoblast progenitors. Development 2006;133:3231–44. [PubMed: 16854976]
17. Glass DA 2nd, Bialek P, Ahn JD, Starbuck M, Patel MS, Clevers H, Taketo MM, Long F, McMahon AP, Lang RA, Karsenty G. Canonical Wnt signaling in differentiated osteoblasts controls osteoclast differentiation. Dev Cell 2005;8:751–64. [PubMed: 15866165]
18. Holmen SL, Zylstra CR, Mukherjee A, Sigler RE, Faugere MC, Bouxsein ML, Deng L, Clemens TL, Williams BO. Essential role of beta-catenin in postnatal bone acquisition. J Biol Chem 2005;280:21162–8. [PubMed: 15802266]
19. Simonet WS, Lacey DL, Dunstan CR, Kelley M, Chang MS, Luthy R, Nguyen HQ, Wooden S, Bennett L, Boone T, Shimamoto G, DeRose M, Elliott R, Colombero A, Tan HL, Trail G, Sullivan J, Davy E, Bucay N, Renshaw-Gegg L, Hughes TM, Hill D, Pattison W, Campbell P, Sander S, Van G, Tarpley J, Derby P, Lee R, Boyle WJ. Osteoprotegerin: a novel secreted protein involved in the regulation of bone density. Cell 1997;89:309–19. [PubMed: 9108485]
20. Jackson A, Vayssiere B, Garcia T, Newell W, Baron R, Roman-Roman S, Rawadi G. Gene array analysis of Wnt-regulated genes in C3H10T1/2 cells. Bone 2005;36:585–98. [PubMed: 15777744]
21. Krishnan V, Bryant HU, Macdougald OA. Regulation of bone mass by Wnt signaling. J Clin Invest 2006;116:1202–9. [PubMed: 16670761]
22. Bodine PV, Zhao W, Kharode YP, Bex FJ, Lambert AJ, Goad MB, Gaur T, Stein GS, Lian JB, Komm BS. The Wnt antagonist secreted frizzled-related protein-1 is a negative regulator of trabecular bone formation in adult mice. Mol Endocrinol 2004;18:1222–37. [PubMed: 14976225]
23. Li X, Zhang Y, Kang H, Liu W, Liu P, Zhang J, Harris SE, Wu D. Sclerostin binds to LRP5/6 and antagonizes canonical Wnt signaling. J Biol Chem 2005;280:19883–7. [PubMed: 15778503]
24. Semenov M, Tamai K, He X. SOST is a ligand for LRP5/LRP6 and a Wnt signaling inhibitor. J Biol Chem 2005;280:26770–5. [PubMed: 15908424]
25. Balemans W, Ebeling M, Patel N, Van Hul E, Olson P, Dioszegi M, Lacza C, Wuyts W, Van Den Ende J, Willems P, Paes-Alves AF, Hill S, Bueno M, Ramos FJ, Tacconi P, Dikkers FG, Stratakis C, Lindpaintner K, Vickery B, Foernzler D, Van Hul W. Increased bone density in sclerosteosis is due to the deficiency of a novel secreted protein (SOST). Hum Mol Genet 2001;10:537–43. [PubMed: 11181578]
26. Brunkow ME, Gardner JC, Van Ness J, Paeper BW, Kovacevich BR, Proll S, Skonier JE, Zhao L, Sabo PJ, Fu Y, Alisch RS, Gillett L, Colbert T, Tacconi P, Galas D, Hamersma H, Beighton P, Mulligan J. Bone dysplasia sclerosteosis results from loss of the SOST gene product, a novel cystine knot-containing protein. Am J Hum Genet 2001;68:577–89. [PubMed: 11179006]
27. Balemans W, Patel N, Ebeling M, Van Hul E, Wuyts W, Lacza C, Dioszegi M, Dikkers FG, Hildering P, Willems PJ, Verheij JB, Lindpaintner K, Vickery B, Foernzler D, Van Hul W. Identification of a 52 kb deletion downstream of the SOST gene in patients with van Buchem disease. J Med Genet 2002;39:91–7. [PubMed: 11836356]
28. Staehling-Hampton K, Proll S, Paeper BW, Zhao L, Charmley P, Brown A, Gardner JC, Galas D, Schatzman RC, Beighton P, Papapoulos S, Hamersma H, Brunkow ME. A 52-kb deletion in the

SOST-MEOX1 intergenic region on 17q12-q21 is associated with van Buchem disease in the Dutch population. Am J Med Genet 2002;110:144–52. [PubMed: 12116252]

29. Semenov MV, He X. LRP5 Mutations Linked to High Bone Mass Diseases Cause Reduced LRP5 Binding and Inhibition by SOST. J Biol Chem 2006;281:38276–84. [PubMed: 17052975]
30. Glinka A, Wu W, Delius H, Monaghan AP, Blumenstock C, Niehrs C. Dickkopf-1 is a member of a new family of secreted proteins and functions in head induction. Nature 1998;391:357–62. [PubMed: 9450748]
31. Mao B, Wu W, Li Y, Hoppe D, Stannek P, Glinka A, Niehrs C. LDL-receptor-related protein 6 is a receptor for Dickkopf proteins. Nature 2001;411:321–5. [PubMed: 11357136]
32. Bafico A, Liu G, Yaniv A, Gazit A, Aaronson SA. Novel mechanism of Wnt signalling inhibition mediated by Dickkopf-1 interaction with LRP6/Arrow. Nat Cell Biol 2001;3:683–6. [PubMed: 11433302]
33. Semenov MV, Tamai K, Brott BK, Kuhl M, Sokol S, He X. Head inducer Dickkopf-1 is a ligand for Wnt coreceptor LRP6. Curr Biol 2001;11:951–61. [PubMed: 11448771]
34. Mao B, Wu W, Davidson G, Marhold J, Li M, Mechler BM, Delius H, Hoppe D, Stannek P, Walter C, Glinka A, Niehrs C. Kremen proteins are Dickkopf receptors that regulate Wnt/beta-catenin signalling. Nature 2002;417:664–7. [PubMed: 12050670]
35. Mukhopadhyay M, Shtrom S, Rodriguez-Esteban C, Chen L, Tsukui T, Gomer L, Dorward DW, Glinka A, Grinberg A, Huang SP, Niehrs C, Belmonte JC, Westphal H. Dickkopf1 is required for embryonic head induction and limb morphogenesis in the mouse. Dev Cell 2001;1:423–34. [PubMed: 11702953]
36. Adamska M, MacDonald BT, Meisler MH. Doubleridge, a mouse mutant with defective compaction of the apical ectodermal ridge and normal dorsal-ventral patterning of the limb. Dev Biol 2003;255:350–62. [PubMed: 12648495]
37. MacDonald BT, Adamska M, Meisler MH. Hypomorphic expression of Dkk1 in the doubleridge mouse: dose dependence and compensatory interactions with Lrp6. Development 2004;131:2543–52. [PubMed: 15115753]
38. Monaghan AP, Kioschis P, Wu W, Zuniga A, Bock D, Poustka A, Delius H, Niehrs C. Dickkopf genes are co-ordinately expressed in mesodermal lineages. Mech Dev 1999;87:45–56. [PubMed: 10495270]
39. Li J, Sarosi I, Cattley RC, Pretorius J, Asuncion F, Grisanti M, Morony S, Adamu S, Geng Z, Qiu W, Kostenuik P, Lacey DL, Simonet WS, Bolon B, Qian X, Shalhoub V, Ominsky MS, Zhu Ke H, Li X, Richards WG. Dkk1-mediated inhibition of Wnt signaling in bone results in osteopenia. Bone 2006;39:754–66. [PubMed: 16730481]
40. Zhang Y, Wang Y, Li X, Zhang J, Mao J, Li Z, Zheng J, Li L, Harris S, Wu D. The LRP5 high-bone-mass G171V mutation disrupts LRP5 interaction with Mesd. Mol Cell Biol 2004;24:4677–84. [PubMed: 15143163]
41. Li X, Liu P, Liu W, Maye P, Zhang J, Zhang Y, Hurley M, Guo C, Boskey A, Sun L, Harris SE, Rowe DW, Ke HZ, Wu D. Dkk2 has a role in terminal osteoblast differentiation and mineralized matrix formation. Nat Genet 2005;37:945–52. [PubMed: 16056226]
42. Morvan F, Boulukos K, Clement-Lacroix P, Roman Roman S, Suc-Royer I, Vayssiere B, Ammann P, Martin P, Pinho S, Pognonec P, Mollat P, Niehrs C, Baron R, Rawadi G. Deletion of a single allele of the Dkk1 gene leads to an increase in bone formation and bone mass. J Bone Miner Res 2006;21:934–45. [PubMed: 16753024]
43. Schmittgen TD. Real-time quantitative PCR. Methods 2001;25:383–5. [PubMed: 11846607]
44. Volkman SK, Galecki AT, Burke DT, Paczas MR, Moalli MR, Miller RA, Goldstein SA. Quantitative trait loci for femoral size and shape in a genetically heterogeneous mouse population. J Bone Miner Res 2003;18:1497–505. [PubMed: 12929939]
45. Favier B, Rijli FM, Fromental-Ramain C, Fraulob V, Chambon P, Dolle P. Functional cooperation between the non-paralogous genes Hoxa-10 and Hoxd-11 in the developing forelimb and axial skeleton. Development 1996;122:449–60. [PubMed: 8625796]
46. Loots GG, Kneissel M, Keller H, Baptist M, Chang J, Collette NM, Ovcharenko D, Plajzer-Frick I, Rubin EM. Genomic deletion of a long-range bone enhancer misregulates sclerostin in Van Buchem disease. Genome Res 2005;15:928–35. [PubMed: 15965026]

47. Wellik DM, Capecchi MR. Hox10 and Hox11 genes are required to globally pattern the mammalian skeleton. Science 2003;301:363–7. [PubMed: 12869760]

48. Hamrick MW, McPherron AC, Lovejoy CO, Hudson J. Femoral morphology and cross-sectional geometry of adult myostatin-deficient mice. Bone 2000;27:343–9. [PubMed: 10962344]

49. Beamer WG, Donahue LR, Rosen CJ, Baylink DJ. Genetic variability in adult bone density among inbred strains of mice. Bone 1996;18:397–403. [PubMed: 8739896]

50. Wergedal JE, Sheng MH, Ackert-Bicknell CL, Beamer WG, Baylink DJ. Genetic variation in femur extrinsic strength in 29 different inbred strains of mice is dependent on variations in femur cross-sectional geometry and bone density. Bone 2005;36:111–22. [PubMed: 15664009]

51. Sheng MH, Lau KH, Mohan S, Baylink DJ, Wergedal JE. High osteoblastic activity in C3H/HeJ mice compared to C57BL/6J mice is associated with low apoptosis in C3H/HeJ osteoblasts. Calcif Tissue Int 2006;78:293–301. [PubMed: 16604280]

52. Sawakami K, Robling AG, Ai M, Pitner ND, Liu D, Warden SJ, Li J, Maye P, Rowe DW, Duncan RL, Warman ML, Turner CH. The Wnt co-receptor LRP5 is essential for skeletal mechanotransduction but not for the anabolic bone response to parathyroid hormone treatment. J Biol Chem 2006;281:23698–711. [PubMed: 16790443]

53. Pinson KI, Brennan J, Monkley S, Avery BJ, Skarnes WC. An LDL-receptor-related protein mediates Wnt signalling in mice. Nature 2000;407:535–8. [PubMed: 11029008]

54. Kokubu C, Heinzmann U, Kokubu T, Sakai N, Kubota T, Kawai M, Wahl MB, Galceran J, Grosschedl R, Ozono K, Imai K. Skeletal defects in ringelschwanz mutant mice reveal that Lrp6 is required for proper somitogenesis and osteogenesis. Development 2004;131:5469–80. [PubMed: 15469977]

55. Mani A, Radhakrishnan J, Wang H, Mani A, Mani MA, Nelson-Williams C, Carew KS, Mane S, Najmabadi H, Wu D, Lifton RP. LRP6 mutation in a family with early coronary disease and metabolic risk factors. Science 2007;315:1278–82. [PubMed: 17332414]

56. Carter M, Chen X, Slowinska B, Minnerath S, Glickstein S, Shi L, Campagne F, Weinstein H, Ross ME. Crooked tail (Cd) model of human folate-responsive neural tube defects is mutated in Wnt coreceptor lipoprotein receptor-related protein 6. Proc Natl Acad Sci U S A 2005;102:12843–8. [PubMed: 16126904]

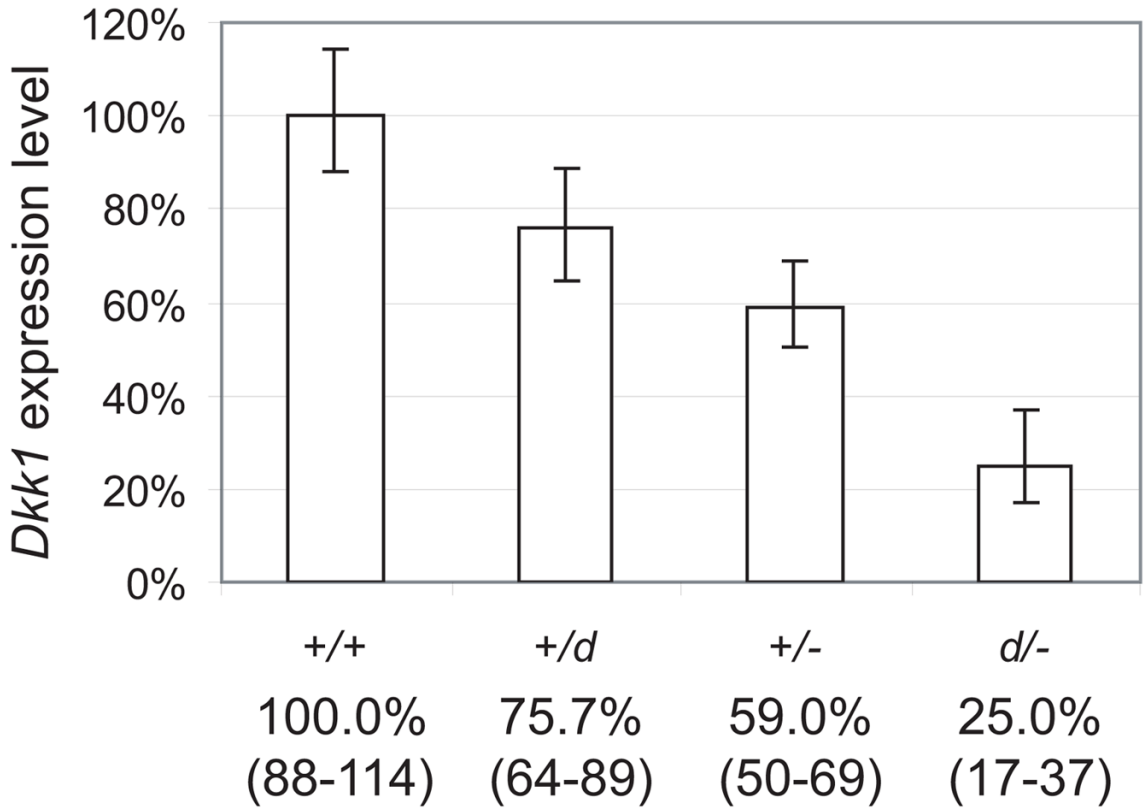

Figure 1.
Genetic titration of *Dkk1* expression levels in mice. Quantitative RT-PCR of *Dkk1* using mRNA from postnatal day 3 calvaria. Average expression levels were normalized to +/+ controls (100%) to assess *Dkk1* levels in the mutant genotypes. Expression level values and the calculated ranges (from ±SD) are displayed below the bars.

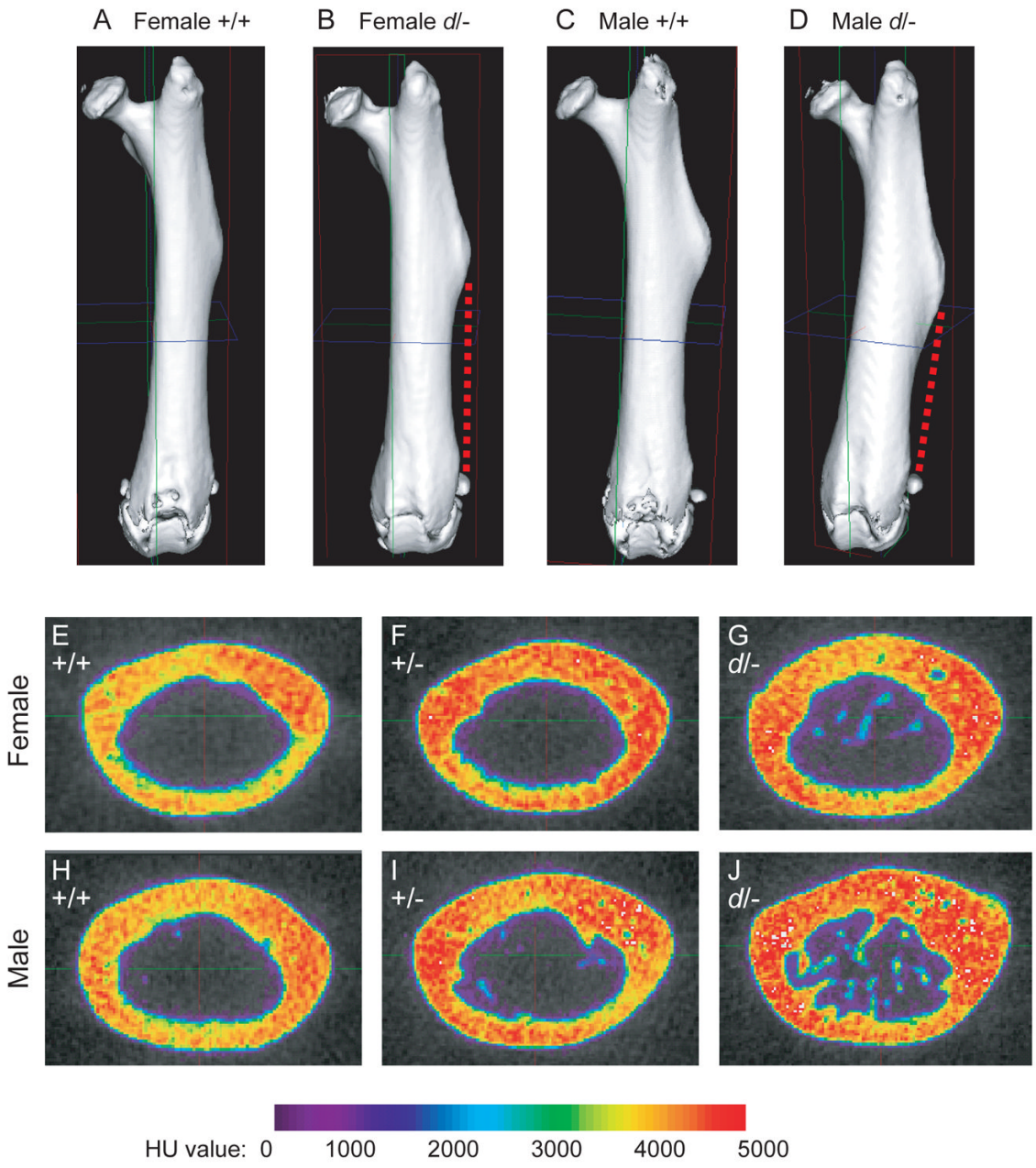

Figure 2.

Altered femur morphology and increased radiodensity in the femur diaphysis in *Dkk1* mutant mice. (A-D) Isosurface images of +/+ and *d*/− scanned left femora oriented to the anterior view to display the position of the third trochanter. Dashed red line indicates the location of the accessory ligament found on *d*/− femora. (E-J) Representative cross section alpha blends from female and male *Dkk1* mutant mice. Radiodensity is expressed in Hounsfield units (HU) based on calibrated HU values for air, water and hydroxyapatite. Note the presence of trabeculae in the mid-diaphysis marrow space.

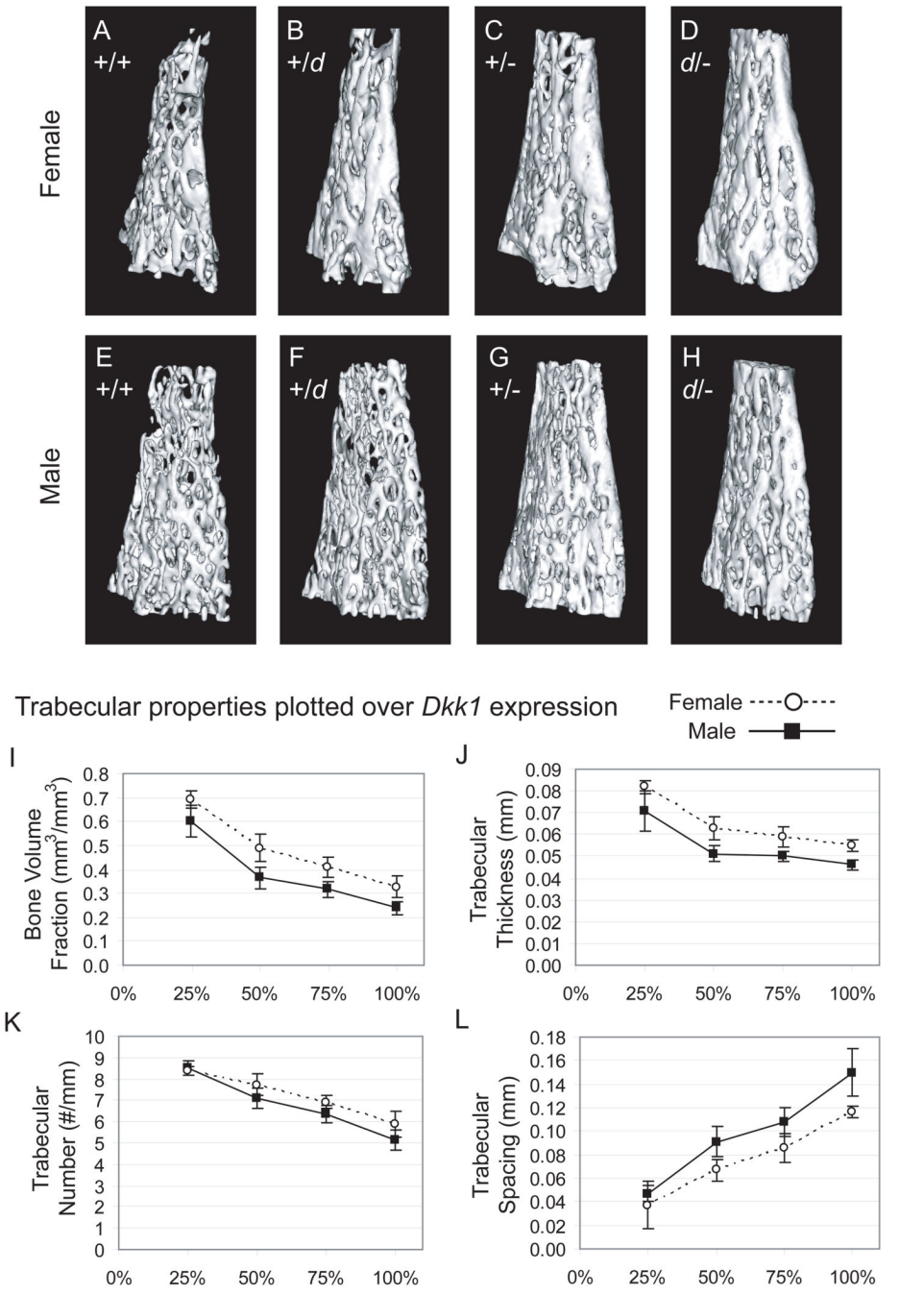

Figure 3.

Reduced *Dkk1* expression increases trabecular bone volume and trabecular number in the *Dkk1* mutant mice. (A-H) Representative trabecular isosurfaces of the distal femur region of interest for female and male mice from each of the *Dkk1* genotypes. (I-L) Graphical representation of the trabecular properties using the *Dkk1* expression levels (*d*/− = 25%, +/− = 50%, +/*d* = 75%, +/+ = 100%) to illustrate the effects of decreasing *Dkk1* amounts.

Table 1

Animal weights and femur characteristics of female and male *Dkk1* mutant mice

	Sample size	Animal weight (g)	Femur length (mm)	Vert. Distance to 3rd Trochanter (mm)	Ratio (femur length/3rd trochanter)
Female					
+/+	**8**	**23.2** ±1.3	**14.77** ±0.17	**9.69** ±0.18	**1.52** ±0.020
+/***d***	**8**	**23.3** ±1.9	**14.77** ±0.31	**9.49** ±0.38	***1.56** ±0.036
+/−	**8**	**22.3** ±1.7	**14.68** ±0.22	***9.42** ±0.29	***1.56** ±0.032
d/−	**4**	**22.2** ±0.9	**14.63** ±0.27	**9.41** ±0.29	***1.55** ±0.022
Male					
+/+	**8**	**29.1** ±2.0	**15.03** ±0.35	**9.68** ±0.34	**1.55** ±0.037
+/***d***	**8**	**29.3** ±3.6	**15.03** ±0.32	****9.58** ±0.30	****1.57** ±0.030
+/−	**8**	**29.0** ±2.6	**15.09** ±0.35	****9.55** ±0.27	****1.58** ±0.017
d/−	**8**	***26.1** ±2.5	***14.74** ±0.15	****8.94** ±0.39	****1.65** ±0.062

For all data, * $p<0.05$ (95% confidence interval) and ** $p<0.01$ (99% confidence interval) compared to +/+ sex matched controls.

Table 2

Cortical bone microCT analysis of the femur diaphysis

	Cortical Thickness (mm)	Cross Sectional Area (mm^2)	Bending Moment of Inertia - Iyy (mm^4)	Tissue Mineral Density (mg/cc)
Female				
+/+	**0.260** ±0.010	**0.869** ±0.035	**0.091** ±0.008	**1099** ±12
+/*d*	**0.268** ±0.010	**0.913** ±0.048	**0.099** ±0.011	**1107** ±11
+/−	***0.280** ±0.017	***0.943** ±0.052	**0.101** ±0.015	**1096** ±11
d/−	****0.307** ±0.015	****1.068** ±0.046	****0.127** ±0.011	**1111** ±21
Male				
+/+	**0.287** ±0.013	**1.033** ±0.038	**0.118** ±0.008	**1106** ±20
+/*d*	**0.298** ±0.007	**1.110** ±0.055	**0.134** ±0.016	**1108** ±13
+/−	***0.307** ±0.014	***1.154** ±0.070	****0.146** ±0.018	**1088** ±14
d/−	****0.358** ±0.014	****1.342** ±0.058	****0.184** ±0.017	**1106** ±16

Table 3

Trabecular bone microCT analysis of the distal femur

	Bone Volume Fraction (mm^3/mm^3)	Trabecular Thickness (mm)	Trabecular Number (#/mm)	Trabecular Spacing (mm)	Tissue Mineral Density (mg/cc)
Female					
+/+	**0.326** ±0.046	**0.055** ±0.0027	**5.89** ±0.59	**0.116** ±0.020	**635** ±14
+/***d***	****0.409** ±0.041	**0.059** ±0.0045	****6.91** ±0.32	****0.086** ±0.009	**649** ±21
+/−	****0.488** ±0.057	****0.063** ±0.0051	****7.71** ±0.51	****0.067** ±0.012	**636** ±15
d/−	****0.691** ±0.038	****0.082** ±0.0030	****8.38** ±0.21	****0.037** ±0.005	**638** ±15
Male					
+/+	**0.239** ±0.028	**0.046** ±0.0021	**5.12** ±0.47	**0.150** ±0.020	**620** ±13
+/***d***	****0.318** ±0.033	**0.050** ±0.0021	****6.35** ±0.43	****0.108** ±0.012	**628** ±13
+/−	****0.365** ±0.047	****0.051** ±0.0036	****7.07** ±0.47	****0.091** ±0.013	***596** ±17
d/−	****0.603** ±0.066	****0.071** ±0.0094	****8.51** ±0.31	****0.047** ±0.007	**625** ±11

Table 4

Intramembranous bone microCT analysis of the calvaria

	Cortical Thickness (mm)	Cross Sectional Area (mm^2)	Bone Mineral Density (mg/cc)	Tissue Mineral Density (mg/cc)
Female				
+/+	**0.229** ±0.072	**0.931** ±0.387	**316** ±87	**534** ±35
+/*d*	**0.212** ±0.046	**0.886** ±0.254	**317** ±61	**527** ±32
+/−	**0.205** ±0.070	**1.023** ±0.329	**285** ±85	**545** ±65
d/−	**0.260** ±0.134	**1.367** ±0.507	**323** ±184	**566** ±19
Male				
+/+	**0.231** ±0.062	**1.108** ±0.727	**341** ±113	**531** ±26
+/*d*	**0.185** ±0.024	**0.646** ±0.266	**278** ±28	**528** ±33
+/−	**0.258** ±0.081	**1.171** ±0.598	**339** ±55	**546** ±60
d/−	**0.206** ±0.072	**1.018** ±0.496	**248** ±90	**561** ±36